Respiratory Medicine Case Reports 9 (2013) 21–26

Contents lists available at SciVerse ScienceDirect

Respiratory Medicine Case Reports

journal homepage: www.elsevier.com/locate/rmcr

Case report

Multidetector computed tomography findings of central bronchopleural fistulas as sequelae of tuberculosis, chemo radiation and trauma: A report of three cases

Ruken Yuksekkaya [a,*], Banu Ozturk [b], Fatih Celikyay [a], Recep Sade [a], Mustafa Kupeli [c], Ali Yeginsu [c]

[a] Gaziosmanpasa University School of Medicine, Department of Radiology, Tokat, Turkey
[b] Gaziosmanpasa University Scool of Medicine, Department of Oncology, Tokat, Turkey
[c] Gaziosmanpasa University School of Medicine, Department of Chest Surgery Tokat, Turkey

ARTICLE INFO

Article history:
Received 21 November 2012
Received in revised form
5 April 2013
Accepted 18 April 2013

Keywords:
Bronchopleural fistula
Multidetector computed tomography
Imaging results

ABSTRACT

A bronchopleural fistula (BPF) is defined as a direct pathway between the bronchial tree or lung parenchyma and the pleural space. Herein, we describe the clinical findings and imaging results of BPFs in three cases. The patients' medical histories revealed that the first had recurrent pulmonary tuberculosis, the second had small-cell lung cancer (SCLC) and had previously undergone chemoradiotherapy, and the third had trauma. Multidetector computed tomography (MDCT) showed clear communication between the airways and pleural spaces which was sufficient for a proper diagnosis without performing a bronchoscopy.

1. Introduction

A bronchopleural fistula (BPF) is a rare condition in which there is a direct passageway between the bronchial tree or lung parenchyma and the pleural space.[1] It can be classified as either central or peripheral.[2] Central types are usually associated with lung resection and trauma while peripheral types are affiliated with necrotizing pneumonia, trauma, lung surgery, and malignancy.[3] In addition, BPFs can cause significant morbidity, prolonged hospitalization, and even death. Therefore, early diagnosis and localization is important for the management of this condition. Multidetector computed tomography (MDCT) is not only useful for detecting the fistula tract, but it can also aid in the determination of the number, size, and location of the fistulas and the identification of any underlying diseases. In this report, the radiological and clinical findings of three cases with BPFs secondary to tuberculosis, chemoradiotherapy, and trauma are reported, respectively. Chest MDCT was an important diagnostic tool in these cases, and further invasive diagnostic procedures, such as bronchoscopies, were not necessary to detect the BPFs.

2. Case reports

2.1. Case 1

A 72-year-old male farmer had been suffering with a cough, hemoptysis, sputum, fever, dyspnea, weakness, and chest pain for 20 days. His medical history indicated that he had been diagnosed with a pulmonary tuberculosis infection 40 years earlier. Furthermore, the patient had relapsed 30 years after the first infection and taken antituberculosis drugs. On clinical examination crackles and reduced breathing sounds in the right hemithorax were detected. Chest radiography showed volume loss, pleural thickening, and a hydropneumothorax on the right side. Also, a mediastinal shift to the right was apparent (Fig. 1). Computed tomography scans were performed with the patients in the dorsal decubitus position during maximum inspiration, and an eight-channel MDCT system (GE Healthcare, Milwaukee, WI, USA) was used. Contiguous axial slices with contrast-enhanced CT scans were undertaken at 5 mm intervals with 5 mm collimation at an automatically modulated amperage of 120 Kvp (120–225 mA). All images were obtained at window levels appropriate for the lung parenchyma (window width, 1500–1700 HU; window level, −600 or −700 HU) and mediastinum (window width, 250–400 HU; window level, 40–50 HU). The images were then reconstructed with a high resolution algorithm, and the multiplanar reformatted (MPR) images were interpreted in various planes. The MDCT revealed a collapsed

* Corresponding author. Tel.: +90 532 7174634; fax: +90 356 2129417.
E-mail addresses: rukenyuksekkaya@yahoo.com (R. Yuksekkaya), drbanutr@yahoo.com (B. Ozturk), fatihcelikyay99@yahoo.com (F. Celikyay), recepsade@yahoo.com (R. Sade), mustafakupeli@yahoo.com (M. Kupeli), aliyeginsu@yahoo.com (A. Yeginsu).

2213-0071
http://dx.doi.org/10.1016/j.rmcr.2013.04.001

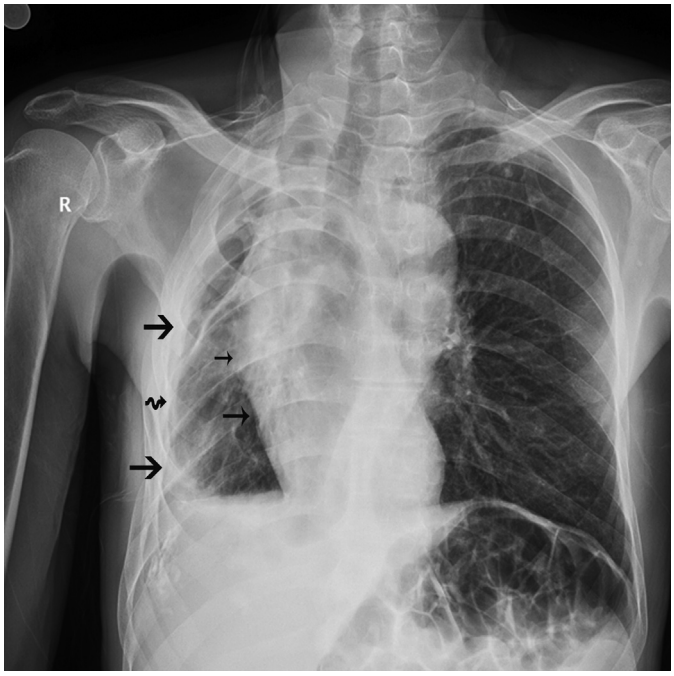

Fig. 1. Chest radiography of the patient at the time of admission showing volume loss, pleural thickening (curved arrow), and a hydropneumothorax (thick arrows) at the right hemithorax. The mediastinal shift to the right is also indicated (thin arrows).

right upper lobe with a mediastinal shift and air-fluid levels. A BPF was visualized in the right upper lobe bronchus on axial, coronal, and oblique coronal MPR images (Figs. 2 and 3). Pleural thickening, calcifications, and enhancement after the administration of contrast material with fluid collection were indicators of empyema (Fig. 4(a)). In addition, a cavitary lesion was present at the superior segment of the right lower lobe (Fig. 4(b)). Peribronchial thickening and cylindrical bronchiectasis in both lungs were detected along with fibrotic changes in the apicoposterior segment of the left upper lobe. The volume of the left lung was increased, and its density was reduced due to air-trapping (Fig. 4(b)). Sputum samples were collected from the patients, and sputum smears for acid-fast bacilli (AFB) and cultures for *Mycobacterium tuberculosis* were obtained as well; however, the samples and cultures were negative. Despite no bacteriological evidence of tuberculosis, the BPF was attributed to chronic inflammation due to tuberculosis and possible tuberculous pleuritis that had been occurring for years. Administration of empirical antibiotics and a mucolytic resolved the patient's symptoms, and he was discharged from the hospital. At the three-month clinical follow-up, his respiratory symptoms had regressed, and chest radiography revealed that the hydropneumothorax and increased volume of the right hemithorax (Fig. 5).

2.2. Case 2

A 62-year-old man was admitted to the oncology department with left chest pain and dyspnea. His past medical history revealed that he had been hospitalized in the intensive care unit (ICU) and been diagnosed with small-cell lung cancer (SCLC) five months prior to admission. A large irregular mass measuring 98 × 63 mm in diameter and enlarged lymphadenopathies of approximately 28 mm in diameter had been found on the left side of the mediastinum via CT at the time of diagnosis. A fiberoptic bronchoscopy had also revealed a mass at the left upper lobe bronchus, and SCLC was diagnosed at the pathological examination of the endobronchial mass. No distant metastasis was revealed via bone scintigraphy or brain and abdominal imaging. The disease was accepted as limited-stage SCLC, and two courses of cisplatin and etoposid were given concomitantly with radiation therapy. After completion, a third course of the same chemotherapy regimen was administered.

The physical examination showed fine crackles on inspiration at the left hemithorax and the breathing sounds were decreased in the left lung. The white blood cell (WBC) count was 10.9×10^9 (neutrophils, 80.9%), the erythrocyte sedimentation rate (ESR) was 120 mm/h, and the C-reactive protein (CRP) level was 205 mg/dL. Chest radiography revealed a loss of volume in the left hemithorax with a mass lesion at the left hilum and an area of consolidation at the left upper and middle zones. There were also alveolar opacities and peribronchovascular thickening on both lungs (Fig. 6(a)). By offering the best supportive care and providing an empirical wide spectrum of antibiotics for pneumonia, the symptoms were resolved, and the patient was discharged from the hospital. However, seven days later, he presented with dyspnea and fever, and chest radiography revealed a collapsed left upper lobe and a pneumothorax on the left side. Segmental and nodular pulmonary infiltrations along

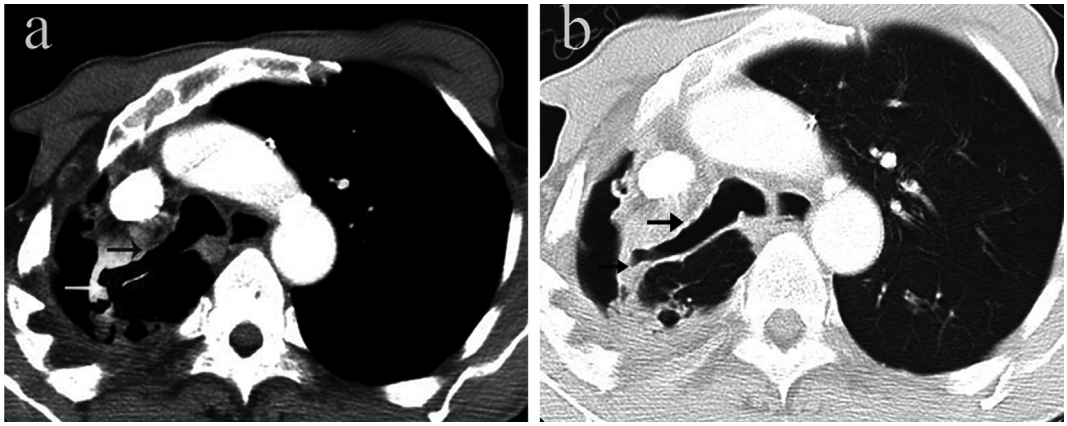

Fig. 2. Axial MDCT images of the patient obtained at (**a**) the mediastinum and (**b**) the lung window settings at the aortic arch level showing the BPF tract as a direct passageway of the right upper lobe bronchus with pleural space (black and white arrows).

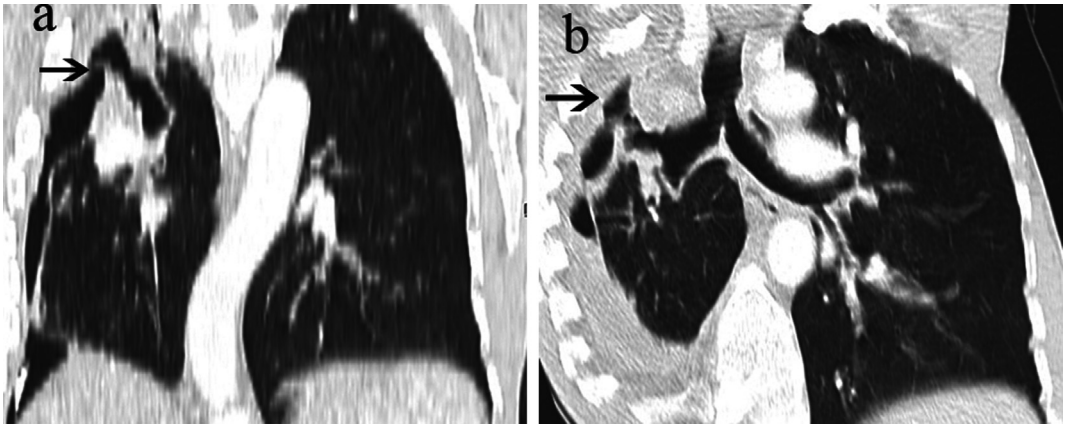

Fig. 3. (**a**) Coronal and (**b**) oblique coronal MPR images of the patient showing the BPF tract (arrows).

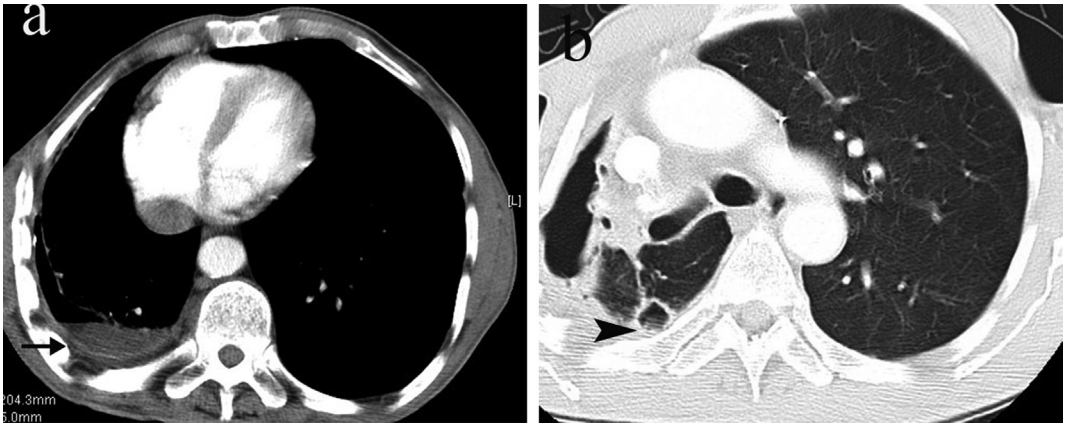

Fig. 4. (**a**) Axial MDCT image of the patient obtained at the mediastinum window setting and cardiac ventricular level showing pleural thickening and enhancement after the administration of contrast material with fluid collection, which are indicators of empyema (arrow). (**b**) Axial MDCT image of the patient at the lung window settings and carina level showing a cavitary lesion at the superior segment of the right lower lobe (arrowhead).

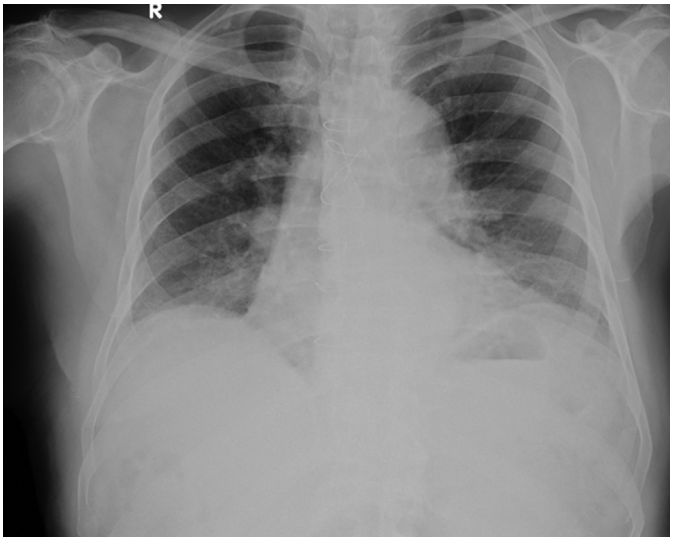

Fig. 5. Chest radiography of the patient three months later demonstrating the resolution of the hydropneumothorax and increased volume of the right hemithorax.

with air-fluid levels and pleural thickening were also observed (Fig. 6(b)). Chest MDCT confirmed the collapsed left upper lobe with air-fluid levels and revealed a mass lesion at the upper lobe bronchus. A BPF in the left upper lobe bronchus was also detected (Fig. 7). Furthermore, pleural thickening with enhancement and effusion were present at the left hemithorax. The area of consolidation (Fig. 7) at the left lung and a cavitary lesion at the superior segment of the left lower lobe were also observed. Additionally, nodular areas of ground glass opacity, cylindrical bronchiectasis with peribronchial thickening, and pleural effusion were identified at the left hemithorax (Fig. 8). The cause of the BPF was accepted as necrotizing pneumonia due to the radiation therapy. The patient refused the insertion of a thorax tube for pleural drainage. Ten days later, he was admitted to the emergency department with mental confusion and respiratory failure. He also had a fever and purulent sputum. The patient was uncooperative and disoriented, and auscultation showed crackles on both hemithoraces. Therefore, he was immediately admitted to the ICU. Despite oxygen inhalation, the use of bronchodilatators, and antibiotic therapy, his clinical course worsened. Cardiopulmonary arrest developed, and the patient died from respiratory failure 12 h after he was taken to the ICU.

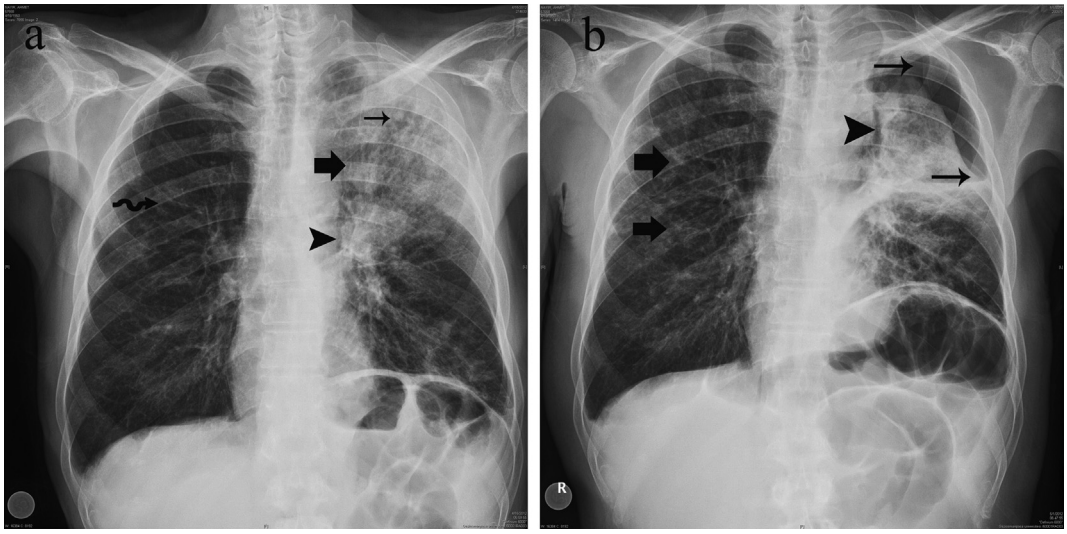

Fig. 6. (**a**) Chest radiography showing the volume loss with a mass lesion at the left hemithorax (arrowhead) and the area of consolidation at the left upper and middle zones (thick arrow). Alveolar opacities and peribronchovascular thickening on both lungs (curved arrow) are shown at the time that the clinical symptoms appeared. (**b**) A collapsed left upper lobe (arrowhead) and a pneumothorax (thin arrows) with air-fluid levels and pleural thickening (thin arrow) on the left side with segmental and nodular pulmonary infiltrations on both sides (thick arrows) are noted at the time of the second admission.

2.3. Case 3

A 16-year-old female patient with an unremarkable medical history was admitted to our emergency department after a fall from three meters. She was conscious, alert, and hemodynamically stable but complained of pain with movement and 4/5 muscle strength in the lower extremities. Auscultation of the lungs showed decreased respiratory sounds at the right hemithorax. Head, spine, and chest MDCT examinations and an abdominal ultrasound examination were done. The head MDCT revealed a subdural hematoma 1 cm in thickness located approximately at the convexity level with no mass effect on the left side and a contusion approximately 2 mm in diameter at the left frontal lobe. There were multiple unstable fractures on the third and fourth vertebrae with compression of the spinal cord. Multiple fracture lines at the spinous and transverse processes, and the laminae of these vertebrae were also observed. In addition, there were hematomas on the right-sided psoas muscle and paravertebral muscles. A chest MDCT examination revealed diffuse, patchy airspace opacities, multiple traumatic hemopneumatoceles with air-fluid levels at the right lower lobe, and a BPF at the right lower lobe bronchus on more than one contiguous slice (Fig. 9). Moreover, a hemopneumothorax with air-fluid levels was detected on the CT scan. The radiological findings were attributed to the type I pulmonary laceration and the formation of a traumatic pneumatocele along with the BPF. The patient then underwent urgent surgery for the stabilization of the lumbar vertebrae fractures and spinal decompression, but the lung laceration and BPF were treated conservatively without any surgical intervention.

3. Discussion

A BPF is a rare but serious complication of lung surgery that is associated with high mortality and morbidity rates. Mortality rates ranging from 18-67% have been reported.[4] The most common cause of death associated with this condition is aspiration pneumonia with subsequent adult respiratory distress syndrome.[5] The etiology of BPF is varied, with the most common cause being postoperative complications from a

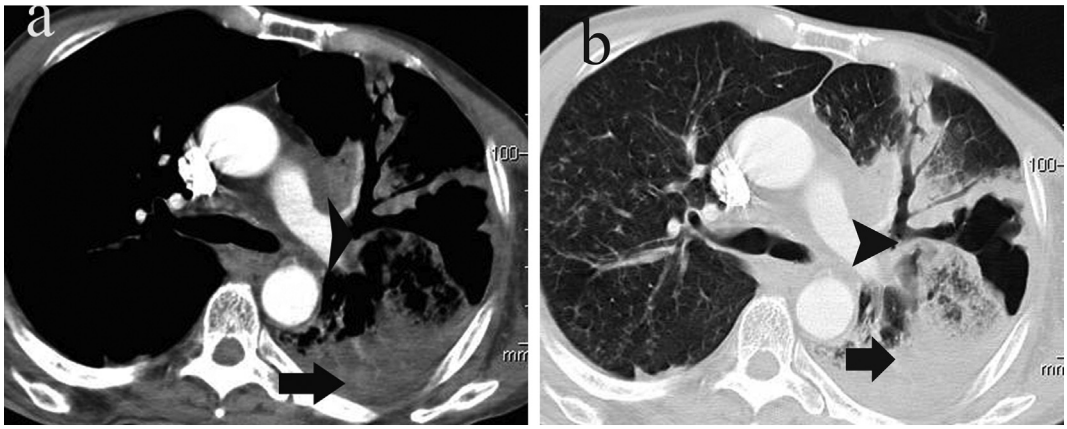

Fig. 7. Axial MDCT images of the patient obtained at (**a**) the mediastinum and (**b**) the lung window settings at the left pulmonary artery level showing the BPF tract at the left upper lobe bronchus (arrowheads) and consolidation at the superior segment of the left lower lobe (thick arrows).

Fig. 8. Axial MDCT image of the patient obtained at the aorticopulmonary level showing pleural thickening with enhancement and effusion (white arrow) at the left hemithorax.

pneumonectomy. Other possibilities include necrotizing pneumonia, empyema, a persistent spontaneous pneumothorax, trauma, radiation therapy, iatrogenic lung cancer, and tuberculosis.[2] However, in the most recent case reports, there was no lung surgery or ventilation treatment. In our patients, the causes of BPF were empyema with destruction and chronic inflammation of tuberculosis that had occurred over a period of years in the first case, radiation therapy with necrotizing pneumonia in the second case, and trauma in the third.

Diagnosis of a BPF is still problematic for radiologists and clinicians because of its rarity. Chest radiography may be useful for detecting a pneumothorax and pleural changes and for evaluating the possibility of a BPF. Furthermore, it can also be helpful for monitoring treatment efficacy.[6] However, it is well known that the fistula tract has never been seen directly on chest radiography,[1] and thin-section MDCT scans with MPR and three-dimensional (3D) reconstruction have been reported to be superior for this purpose.[7,8] The diagnostic value of conventional and single-detector CT scanners have been demonstrated in several studies, especially with regard to peripheral BPF.[1,9,10] There has been only one study regarding MDCT findings of a BPF in the literature,[6] but a limited number of case reports do exist.[8,11] Multidetector CT is a non-invasive and cost-effective method for evaluating the presence, location, and size of a BPF. In fact, a peripheral BPF can be localized with MDCT if there is a distinct channel between the lung or a peripheral bronchus and the pleura.[10] The underlying causes for BPFs can also be evaluated with MDCT. It provides thin-section imaging with overlapping reconstruction. The ability to evaluate the lungs in more than one plane with MPR images is another important advantage of MDCT. This is especially true in the coronal plane because of the many airways that run perpendicular to the axial plane.[7] The MPR and 3D images available with the MDCT are also beneficial during BPF management. Ricci et al.[10] suggested that CT could be used as a guide in surgical procedures by identifying and localizing the peripheral BPF or its probable cause. However, they did no show a statistically significant advantage when utilizing thin-section CT in their study group composed of 33 patients. Wescott and Wolpe[9] concluded that both standard and thin-section CT are important for detecting BPFs, and Seo et al.[7] suggested that thin-section MDCT with axial and MPR images was important in the detection of small, central BPFs. Standard CT images are at a disadvantage due to the plugging of the fistula with debris or secretions and the small size of the defect.[7] Multidetector CT scanners can solve these problems with their thin sections, faster scanning times, fewer respiration artefacts, and higher image quality.

In our patients, MDCT scans were performed before bronchoscopies and other traditional methods, and BPF tracts together with their sizes and locations were clearly demonstrated. Thus, more invasive methods such as bronchoscopies or thorachoscopies were not necessary. In addition, the MPR images were helpful for viewing the entire fistula tract.

Chest MDCT is an accurate, easy, and non-invasive technique for diagnosing and monitoring BPFs and should be the first diagnostic method of choice for patients who are clinically suspected of having a BPF. Multidetector CT allows for the evaluation of the presence, size, and localization of the fistula tract and also demonstrates the possible underlying causes of this rare occurrence.

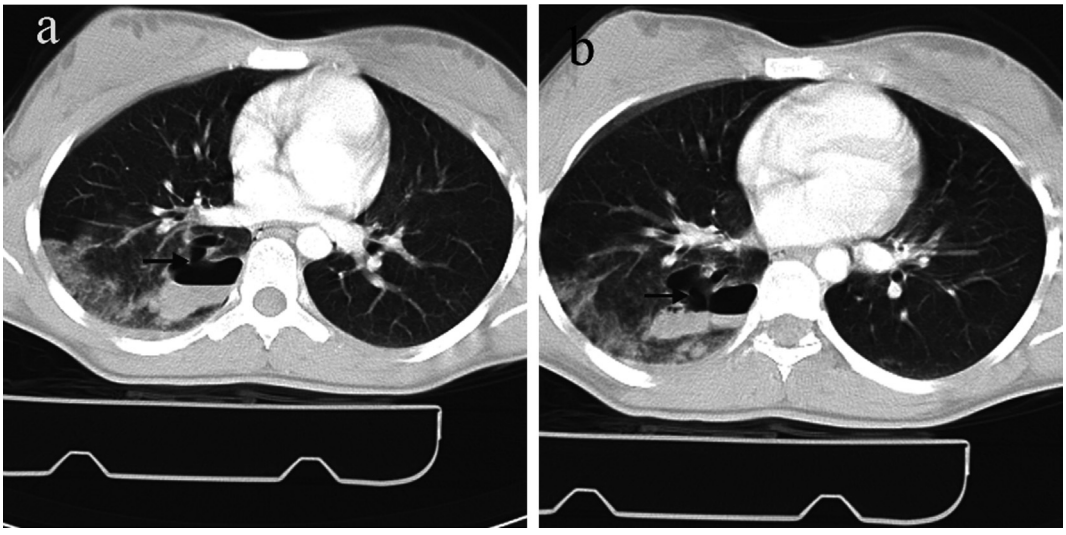

Fig. 9. Axial MDCT image of the patient obtained at (**a**) the pulmonary vein and (**b**) at the cardiac ventricular level showing the BPF tract at the right lower lobe bronchus (arrows).

Funding

The authors received no financial support for the research and/or authorship of this article.

Conflict of interest

There is no conflicts of interests that authors have to be declared

References

1. Stern EJ, Sun H, Haramati LB. Peripheral bronchopleural fistulas: CT imaging features. *AJR Am J Roentgenol* 1996;**167**:117–20.
2. Hsu JT, Bennett GM, Wolff E. Radiologic assessment of bronchopleural fistula with emphyema. *Radiology* 1972;**103**:41–5.
3. Lois M, Noppen M. Bronchopleural fistulas: an overview of the problem with special focus on endoscopic management. *Chest* 2005;**128**:3955–65.
4. Hollaus PH, Lax F, el-Nashef BB, Hauck HH, Lucciarini P, Pridun NS. Natural history of bronchopleural fistula after pneumonectomy: a review of 96 cases. *Ann Thorac Surg* 1997;**63**:1391–6.
5. Kim EU, Lee KS, Shim YM, Kim J, Kim K, Kim TS, et al. Radiographic and CT findings in complications following pulmonary resection. *Radiographics* 2002;**22**:67–86.
6. Choi JA, Hong KT, Oh YW, Chung MH, Seol HY, Kang EY. CT manifestations of latesequelae in patients with tuberculouspleuritis. *AJR Am J Roentgenol* 2001;**176**:441–5.
7. Seo H, Kim TJ, Jin KN, Lee KW. Multi-detector row computed tomography evaluation of bronchopleural fistula: correlation with clinical, bronchoscopic, and surgical findings. *J Comput Assist Tomogr* 2010;**34**:13–8.
8. Shah, Marwah R, Talwar I. Diagnosis of bronchopleural fistula with thin section CT scans. *Bombay Hosp J* 2010;**52**:254–6.
9. Wescott JL, Volpe JP. Peripheral bronchopleural fistula: CT evaluation in 20 patients with pneumonia, emphyema, or postoperative air leak. *Radiology* 1995;**196**:175–81.
10. Ricci ZJ, Haramati LB, Rosenbaum AT, Liebling MS. Role of computed tomography in guiding the management of peripheral bronchopleural fistula. *J Thorac Imaging* 2002;**17**:214–8.
11. Vogel N, Wolcke B, Kauczor HU, Kelbel C, Mildenberger P. Detection of bronchopleural fistula with spiral CT and 3D reconstruction. *Aktuelle Radiol* 1995;**5**:176–8.